

Relationships between selective neuronal loss and microglial activation after ischemic stroke in man

Journal:	<i>Brain</i>
Manuscript ID	BRAIN-2017-01332.R1
Manuscript Type:	Original Article
Date Submitted by the Author:	n/a
Complete List of Authors:	Morris, Rhiannon; University of Cambridge, Dept of Clinical Neurosciences Jones, P Simon; University of Cambridge, Clinical Neurosciences Alawneh, Josef; University of Cambridge Clinical Neurosciences Hong, Young; University of Cambridge, Department of Clinical Neurosciences Fryer, Tim; University of Cambridge Clinical Neurosciences Aigbirhio, Franklin; University of Cambridge Clinical Neurosciences Warburton, Elizabeth; University of Cambridge, Clinical Neurosciences Baron, Jean-Claude; University of Cambridge, Dept of Clinical Neurosciences; INSERM U894, Université Paris Descartes
Subject category:	CNS injury and stroke
To search keyword list, use whole or part words followed by an *:	Cerebral ischaemia < CNS INJURY AND STROKE, Stroke: imaging < CNS INJURY AND STROKE, Cerebral blood flow < CNS INJURY AND STROKE, Cerebral infarction < CNS INJURY AND STROKE, Stroke: other < CNS INJURY AND STROKE

SCHOLARONE™
 Manuscripts

Relationships between selective neuronal loss and microglial activation after ischemic stroke in man

Rhiannon S. Morris¹, P. Simon Jones¹, Josef A. Alawneh¹, Young T. Hong², Tim D. Fryer², Franklin I. Aigbirhio², Elizabeth A. Warburton¹, Jean-Claude Baron^{1,3}.

1. Stroke Research Group, Dept of Clinical Neurosciences, University of Cambridge, UK
2. Wolfson Brain Imaging Centre, Dept of Clinical Neurosciences, University of Cambridge, UK
3. Dept of Neurology, Sainte-Anne Hospital, Paris Descartes University, Inserm U894, Paris, France

Correspondance:

Prof Jean-Claude Baron, Dept of Neurology, Sainte-Anne Hospital, 1 rue Cabanis, 75014, Paris, France ; email: jean-claude.baron@inserm.fr

Running title: Neuronal loss and microglia in penumbra

Word count:

Core text: 6,000

Abstract: 400

Figures: 3 (colour: 2)

Tables: 4

Abstract

Modern ischaemic stroke management involves intravenous thrombolysis followed by mechanical thrombectomy, which allows markedly higher rates of recanalization and penumbral salvage than thrombolysis alone. However, <50% of treated patients eventually enjoy independent life. It is therefore important to identify complementary therapeutic targets. In rodent models, the salvaged penumbra is consistently affected by selective neuronal loss, which may hinder recovery by interfering with plastic processes, as well as by microglial activation, which may exacerbate neuronal death. However, whether the salvaged penumbra in man is similarly affected is still unclear. Here we determined whether these two processes affect the non-infarcted penumbra in man and, if so, whether they are inter-related.

We prospectively recruited patients with i) acute middle-cerebral artery stroke; ii) penumbra present on CT perfusion obtained <4.5hrs of stroke onset; and iii) early neurological recovery as a marker of penumbral salvage. Positron-emission tomography with both ^{11}C -Flumazenil and ^{11}C -PK11195, as well as magnetic resonance imaging to map the final infarct, were obtained at pre-defined follow-up times. The presence of selective neuronal loss and microglial activation was determined voxel-wise within the magnetic-resonance imaging normal-appearing ipsilateral non-infarcted zone and surviving penumbra masks, and their inter-relationship was assessed both across and within patients. Dilated infarct contours were consistently excluded to control for partial volume effects.

Across the 16 recruited patients, there was reduced ^{11}C -Flumazenil and increased ^{11}C -PK11195 binding in the whole ipsilateral non-infarcted zone ($p=0.04$ and 0.02 , respectively). Within the non-infarcted penumbra, ^{11}C -Flumazenil was also reduced ($p = 0.001$), without clear increase in ^{11}C -PK11195 ($p=0.18$). There was no significant correlation between ^{11}C -Flumazenil and ^{11}C -PK11195 in either compartment.

This mechanistic study provides direct evidence for the presence of both neuronal loss and microglial activation in the ipsilateral non-infarcted zone. Further, we demonstrate the presence of neuronal loss affecting the surviving penumbra, with no or only mild microglial activation, and no significant relationship between these two processes. Thus, microglial activation may not contribute to penumbral neuronal loss

in man, and its presence in the ipsilateral hemisphere may merely reflect secondary remote degeneration. Selective neuronal loss in the surviving penumbra may represent a novel therapeutic target as an adjunct to penumbral salvage to further improve functional outcome. However, microglial activation may not stand as the primary therapeutic approach. Protecting the penumbra by e.g. improving perfusion and oxygenation in conjunction with thrombectomy may be a better approach. ^{11}C -Flumazenil PET would be useful to monitor the effects of such therapies.

Key words: PET, ^{11}C -PK11195, ^{11}C -Flumazenil, acute stroke, recovery, cerebral ischemia, imaging, cerebral infarction, cerebral blood flow

For Peer Review

Introduction

The ischaemic penumbra represents the main target for acute stroke therapy (Muir *et al.*, 2006), and preventing it from progressing to infarction enhances neurological recovery (Furlan *et al.*, 1996, Heiss *et al.*, 1998). Reperfusion therapies, namely intravenous thrombolysis and mechanical thrombectomy, are now licensed to salvage the penumbra, which has revolutionized stroke management. In spite of these breakthroughs, however, **functional outcome remains poor (i.e., lost independence) in the majority of treated patients, even despite the >80% recanalization rate afforded by thrombectomy** (Emberson *et al.*, 2014, Goyal *et al.*, 2016). There is therefore an urgent need to identify novel therapeutic targets so as to improve functional recovery in successfully recanalized stroke patients (Fisher and Saver, 2015).

In animal models the salvaged penumbra is consistently affected by selective neuronal loss (SNL) and resident microglia activation (MA) (for review see (Baron *et al.*, 2014)), and even isolated SNL at least transiently impacts sensorimotor performance (Sicard *et al.*, 2006, Balkaya *et al.*, 2013, Ejaz *et al.*, 2015). Thus, SNL may hinder recovery by restricting neuronal plasticity in peri-infarct tissue, an area considered critical for recovery of lost functions (Cao *et al.*, 1999, Cramer *et al.*, 2000, Calautti and Baron, 2003, Jaillard *et al.*, 2005, Nudo, 2006). Accordingly, SNL may represent a novel therapeutic target for stroke. However, as it may exacerbate SNL via release of neurotoxic cytokines, MA might in fact represent the prime therapeutic target (Kaushal and Schlichter, 2008, Kriz and Lalancette-Hebert, 2009, Hu *et al.*, 2012, Baron *et al.*, 2014). This notion is supported by the finding in rodents of significant correlations between SNL and MA in the surviving penumbra (Hughes *et al.*, 2010, Hughes *et al.*, 2012). However, causality could just as well go in reverse given that MA is initially triggered by neuronal death (Schwartz, 2003, Kriz and Lalancette-Hebert, 2009). Alternatively, therefore, SNL could result from other mechanisms, such as delayed ischemic and/or reperfusion-related early neuronal death.

At this point, however, the key issue with respect to clinical relevance is whether the surviving penumbra is also affected by SNL and MA in man, and if so, whether these two processes are correlated, which would point to MA as primary target. To address these issues, and eventually identify target populations for drug

trials, sensitive and selective imaging markers are required. Owing to the normality of conventional structural MRI in areas affected by SNL and MA in rodents (Li *et al.*, 1999, Sicard *et al.*, 2006, Sicard *et al.*, 2006, Wegener *et al.*, 2006, Ejaz *et al.*, 2013, Ejaz *et al.*, 2015), radiolabeled tracers have been employed so far. Prominent among these are the positron emission tomography (PET) ligands ^{11}C -Flumazenil (FMZ) and ^{11}C -[R]-PK11195 (PK), respectively, both recently validated in rodent models as selective *in vivo* markers against post-mortem immunohistochemistry (Hughes *et al.*, 2012, Ejaz *et al.*, 2013), **confirming earlier *in vitro* studies showing co-localization of ^3H -labelled PK and FMZ with activated microglia and SNL, respectively** (Myers *et al.*, 1991, Stephenson *et al.*, 1995, Katchanov *et al.*, 2003).

Few clinical stroke studies have so far investigated these issues. Although an FMZ-PET study documented the presence of SNL in the non-infarcted MCA territory, it did not directly assess the surviving penumbra *per se* (Guadagno *et al.*, 2008). Two other studies using ^{123}I -Iomazenil (IMZ) single-photon emission tomography (SPECT) suggested the presence of SNL in the NIP (Nakagawara *et al.*, 1997, Saur *et al.*, 2006), but have limitations. The tracer IMZ is suboptimal due to very slow tissue kinetics making its uptake and subsequent binding dependent on perfusion (Videbaek *et al.*, 1993, Videbaek *et al.*, 1995), and furthermore in one study IMZ brain uptake was measured at an early post-injection timepoint (Saur *et al.*, 2006), likely exaggerating this perfusion dependence. The poor spatial resolution of SPECT may cause the low IMZ uptake present in infarcted areas to contaminate peri-infarct areas, in turn overestimating SNL. Also, in one study (Saur *et al.*, 2006), SPECT was performed 5-15 days post-stroke, when blood-brain barrier disruption is at its peak, while in the other the IMZ images were not coregistered with follow-up structural images (Nakagawara *et al.*, 1997), preventing direct assessment of IMZ uptake in the surviving penumbra. A recent small-scale (n=7 patients) FMZ-PET study also from our group that assessed FMZ binding in relation to fMRI activation clusters reported a significant FMZ binding reduction in the non-activated part, but not the activated part, of the surviving penumbra (Carrera *et al.*, 2013). Finally, a recent study using sophisticated cortex flattening methodology found reduced FMZ binding in the immediate peri-infarct area (Funck *et al.*, 2017), but the relevance of this finding to the penumbra is unclear as acute-stage perfusion mapping was not part of this study.

Overall, therefore, although there is strong evidence of SNL in the non-infarcted MCA territory, whether it affects the surviving penumbra *per se* remains unsettled.

Even fewer clinical studies have thus far assessed MA in non-infarcted tissue following MCA stroke, and none specifically the surviving penumbra. Two studies using PK-PET documented inflammation along the degenerating cortico-spinal tract (Radlinska *et al.*, 2009, Thiel *et al.*, 2010), and another (Pappata *et al.*, 2000) in the ipsilateral thalamus, which the authors attributed to Wallerian and/or retrograde thalamo-cortical degeneration as readily observed in rodents (Dubois *et al.*, 1988, Tamura *et al.*, 1991, Rupalla *et al.*, 1998, Arlicot *et al.*, 2010, Walberer *et al.*, 2014). In a study of six patients in whom PK-PET was performed 3-14 days post-stroke (Gerhard *et al.*, 2005), MA was found in the non-infarcted ipsilateral hemisphere in four. However, as no measures were taken to control for the smearing of high within-infarct PK uptake onto neighbouring areas, the validity of these findings is uncertain. Like in the above-mentioned studies, these authors also documented MA in connected areas of the ipsilateral hemisphere and thalamus and pons bilaterally, again attributing it to remote degeneration. In a small-scale study from our group where immediate peri-infarct areas were excluded from the analysis by applying infarct mask dilatation (Price *et al.*, 2006), MA was found in the non-infarcted affected MCA territory in three patients. Taken together, there is preliminary evidence for the presence of MA in the non-infarcted MCA territory, however no study so far has assessed MA within the surviving penumbra *per se*.

We therefore designed the present mechanistic study to address two main unanswered questions: i) is the non-infarcted penumbra affected by SNL and MA in man? ; and ii) does a quantitative correlation exist between these two processes? Based on the above evidence, we predicted the answer to both questions would be positive.

To test these hypotheses, we prospectively enrolled a sizeable sample of acute MCA stroke patients with documented penumbra on admission CT perfusion (CTp) as well as early neurological improvement (ENI) as a marker of penumbral salvage, to undergo both PK and FMZ PET in the subacute/early chronic stage, and follow-up MRI to map the final infarct.

Material and Methods

Patients

We prospectively recruited adult subjects i) admitted within 6hrs of onset (or last-time-seen-well) of first-ever MCA stroke; ii) with admission NIHSS ≥ 2 (or isolated aphasia); iii) in whom admission CT perfusion (CTp) documented the presence of penumbra; and iv) **who experienced ENI, defined as a gain in National Institute of Health Stroke Scale (NIHSS) score ≥ 8 within the first 24 hours or NIHSS ≤ 2 at 24 hours (Saver, 2011), suggesting penumbral salvage. Eligible candidates were approached for consentment only after routine 24hrs NIHSS assessment and post-processing of the admission CTp data had provided evidence of ENI and penumbra, respectively. Assessment of recanalization, which is not part of routine stroke management, did not belong in the study's imaging protocol. Exclusion criteria are listed in **Supplemental Material**.**

Clinical assessment

Standard clinical data (age, gender, baseline observations, past medical history, vascular risk factors, drug and alcohol history, medications on admission and discharge, acute interventions for stroke administered and cause of stroke) were recorded for each recruited patient. Clinical course was determined by serial NIHSS measurements obtained on admission, at 24hrs and at each follow-up PET visit.

Age-matched healthy controls

To obtain normative values, stroke-age healthy volunteers were recruited and underwent either the FMZ or the PK scan (12 and 10 subjects, of gender (F/M) and mean \pm SD 6/6 and 3/7, and 61 ± 8 and 60 ± 7 yrs, respectively). Exclusion criteria appear in **Supplemental Material**

The Cambridgeshire Research Ethics Committee and the UK Administration of Radioactive Substances Advisory Committee approved this study. Written informed consent to participate was obtained from all subjects.

CT perfusion

As part of standard clinical care, non-contrast CT (NCCT) and CTp were acquired in immediate succession during the hyper-acute phase, in the same orientation. See **Supplemental Material** for scanning procedures.

PET

Patients underwent both PK and FMZ PET, respectively in the subacute (day 13-28, counting stroke day as day 0) and early chronic (6-21 weeks) post-stroke stage. For PK this time window relied on previous clinical studies showing it to be optimal for post-stroke MA (Sette *et al.*, 1993, Gerhard *et al.*, 2005, Price *et al.*, 2006). For FMZ it was chosen to allow post-stroke SNL to become established (Nakagawara *et al.*, 1997, Guadagno *et al.*, 2008). Note that SNL, once established, is stable (Sette *et al.*, 1993, Nakagawara *et al.*, 1997), whereas post-stroke MA is transient (Ramsay *et al.*, 1992, Sette *et al.*, 1993, Price *et al.*, 2006).

Details on PET scanning procedures are provided in **Supplemental Material**.

MRI

Scans were performed immediately prior to or after each PET scanning session. **Details on sequences used appear in Supplemental Material.**

Image processing and data analysis

CT perfusion

The procedures, including the identification of penumbral voxels, followed those previously published in detail by our group (Guadagno *et al.*, 2008, Alawneh *et al.*, 2011, Carrera *et al.*, 2013), and are presented in **Supplemental Material**.

Infarct map and PET-MR image co-registration

The final infarct was manually outlined on the FLAIR images (**with help from inspection of corresponding T1 images whenever judged useful**) by an experienced neurologist and imaging scientist (JCB) blinded to the clinical data (see **Figure 1** for an illustration). PET-MR coregistration was carried out as detailed previously (Guadagno *et al.*, 2008, Alawneh *et al.*, 2011, Carrera *et al.*, 2013). Further information is available in **Supplemental Material**.

PET

Binding potential (BP_{ND}) maps were generated voxel-wise for both FMZ and PK, using the basis function version of the simplified tissue reference model (STRM) (Lammertsma and Hume, 1996, Gunn *et al.*, 1997) in Receptor Parametric Mapping (RPM) software, which controls for tracer entry in brain tissue. See **Supplemental Material** for further details.

Mapping SNL and MA within the ultimately non-infarcted MCA territory

Note that CTp data were not used for this analysis.

FMZ: voxel-based single-subject analysis

We aimed to map and count, in each patient relative to the group of normal controls, the voxels with significantly reduced FMZ BP_{ND} present within the affected-side MCA territory but outside the final infarct, as well as within the mirror mask in the unaffected hemisphere. This was accomplished by applying a single-subject voxel-wise analysis, which followed the methodology originally published by Signorini *et al.* (Signorini *et al.*, 1999) and detailed in Guadagno *et al.* (Guadagno *et al.*, 2008) and in **Supplemental Material.**

PK: voxel-based single-subject analysis

The individual-subject SPM analysis implemented for FMZ was not applicable to the PK data because PK BP_{ND} values, expressed relative to the cerebellum, are close to zero in normal brain tissue, with negative as well as positive values. We

therefore applied the method previously used in Price et al (Price *et al.*, 2006) and detailed in **Supplemental Material**.

In order to increase sample size, two of the four patients previously reported by Price et al (Price *et al.*, 2006), whose PK study was within the same time-window as the present study (pts 1 and 2 of their Table 1; PK studies carried out day 13 and day 25 post-stroke, respectively) were included in the present analysis. Apart from not undergoing a CTP on admission, and therefore being ineligible for the subsequent analyses regarding the NIP, these two patients were similar to the rest in terms of admission NIHSS and 24hrs recovery, see Table 2.

Mapping SNL and MA within the non-infarcted penumbra (NIP)

For this analysis, all three imaging modalities, namely PET, MR and acute-stage CTP, were used in conjunction and co-registration. Image processing details are provided in **Supplemental Material**. Given the ‘pixellated’ nature of the NIP mask and the required cross-modalities image co-registration to native PET space, the voxel-based analysis described above for the non-infarcted MCA masks was not applicable. Instead, the FMZ and PK BP_{ND} values across all voxels belonging in the NIP and mirror NIP masks were extracted in each subject, and compared across patients for statistical significance.

Relationship between SNL and MA

The relationship between SNL and MA was determined by correlation analyses, first within the non-infarcted MCA territory (both across the sample and individually), and then within the NIP proper across the sample. See **Supplemental Material** for details.

Statistical analysis

To test the hypothesis that SNL (or MA) is present in the non-infarcted MCA territory, we assessed across the sample whether the number of FMZ (or PK) BP_{ND} voxels within the non-infarcted MCA mask that survived the statistical threshold

determined in the healthy controls was significantly higher than the corresponding voxel number in the mirror mask, as described elsewhere (Price *et al.*, 2006, Guadagno *et al.*, 2008). To test this difference, non-parametric Wilcoxon signed-rank tests were used given the intrinsic zero-voxel floor effect (i.e., no surviving voxel) intrinsically skewing the distribution, and the wide distribution of actual voxel numbers exposing to the risk of outliers (see Table 3). Comparing the two hemispheres aimed to account for potential non-specific, bilaterally distributed changes in binding sites in the stroke population studied, either pre-morbid or secondary to stroke-related diffuse effects such as Wallerian degeneration (Gerhard *et al.*, 2005, Guadagno *et al.*, 2008). To investigate whether age, time from onset to PET data acquisition or final infarct volume influenced the results, non-parametric correlation between the inter-hemispheric difference in significant voxel numbers and these potential confounders were also assessed.

To test the hypothesis that significant SNL affects the NIP, we assessed whether, across patients, the individual mean FMZ BP_{ND} values within the NIP mask was significantly higher than that in the mirror mask, again using non-parametric Wilcoxon signed-rank tests given the small sample and the risk of outliers. The same procedure was repeated for PK BP_{ND} values.

Two-tailed $P < .05$ was regarded as significant throughout.

Results

Patients

Out of 29 eligible patients, 10 declined to volunteer for the study and 19 consented. One patient subsequently withdrew consent, and PET studies failed in another two, leaving a total of 16 patients effectively included. In the same period, 229 pts underwent CTp in our centre as potential candidates for thrombolysis, of which 152 had a final diagnosis of anterior circulation stroke.

The main demographics and clinical data of the 16 included patients are presented in **Table 1**. There were 9 males and 7 females, median age was 66yrs and median admission NIHSS was 12 (range 3-21). Twelve patients were thrombolysed, and none thrombectomized. **Table 2** shows the NIHSS scores at admission, 24hrs and time of the PET scans, as well as the stroke-to-PET delays and infarct volume.

PET scanning

Fifteen patients successfully underwent FMZ-PET, 14 PK-PET and 13 both scans (**Table 2**). Both scans were not performed in three patients because of failed PK synthesis within the prescribed time-window (n=2) and withdrawal from the study after FMZ-PET (n=1; this patient however agreed to let us use her PK dataset).

SNL and MA in the non-infarcted MCA territory

FMZ:

Out of 15 patients, seven showed a greater number of voxels surviving the cut-off in the affected than unaffected hemisphere - often markedly so -, two had mildly higher voxel number in the unaffected hemisphere, and six had no significant voxels in either hemisphere (**Table 3**). This distribution was statistically significant in favour of the affected hemisphere (Wilcoxon signed-rank test, $z = -2.073$, $p = .039$, $r = 0.60$; number of significant voxels: median_{affected} =101 vs median_{unaffected} =0). **Figure 2** illustrates typical SPM findings across several brain slices in the same patient as shown in Figure 1, depicting the expected 'patchy' pattern of significant FMZ binding loss across the non-infarcted cortical MCA territory. See **Supplemental Material** for further results.

PK:

The PK ratio was larger in the affected than unaffected hemisphere in 12/16 patients (**Table 3**), and across patients significantly increased on the affected hemisphere compared to the unaffected (median= 2.2% vs 1.5%; $p= 0.021$, Wilcoxon signed-rank test). In addition, the (affected – unaffected) inter-hemispheric (A-U) PK ratio difference was significantly larger in patients as compared to the 10 controls (median = 5.5 and 0.08%, respectively; $p=0.008$, Mann-Whitney test). Individually, the (A-U) difference in PK ratio was beyond the upper 95% confidence limit for inter-hemispheric difference derived from the the 10 controls in 11/16 patients (see **Table 3** for details).

FMZ-PK relationship within the non-infarcted MCA mask (n=13)

There was no significant correlation between interhemispheric (A-U) difference in number of FMZ and PK significant voxels ($\tau = -0.128$, $p = 0.56$). In the within-subject analysis, the correlation between FMZ BP_{ND} A/U ratio and PK BP_{ND} (A-U) difference did not reach statistical significance in any patient.

SNL and MA within the non-infarcted penumbra (NIP)

Table 4 shows for each subject the mean FMZ and PK BP_{ND} values in the NIP and mirror NIP masks, the mean FMZ A/U ratio and the mean PK (A – U) difference.

FMZ

All 15 subjects who underwent an FMZ study had a lower mean FMZ BP_{ND} in the NIP compared to the mirror NIP, a statistically significant distribution (median_{NIP} = 2.76 and 3.15, respectively; Wilcoxon signed-rank test, $z = -3.408$, $p = 0.001$).

PK

Nine/14 patients had a higher mean PK BP_{ND} in the NIP compared to the mirror NIP (median = -0.0926 vs -0.115, respectively), however this difference did not reach statistical significance (Wilcoxon signed-rank test, $z = 1.35$, $p = .177$).

Despite this negative finding across patients, visual inspection of the individual image datasets suggested the presence of increased PK binding within cortical NIP in three patients (# 2, 9 and 16). **Figure 1** illustrates for a single axial plane from patient 2 the presence of increased PK binding in the cortical NIP (yellow

arrows), associated with reduced FMZ binding (red arrows). Accordingly, this patient had the highest (A-U) PK difference in the NIP (Table 4), along with the second lowest FMZ (A/U) ratio. The (A-U) PK difference in the other two patients was however unremarkable. Note that comparing these values to normative data was not feasible, as mimicking the NIP mask in the control subjects was deemed impossible, or far too inaccurate.

Relationship between SNL and MA within the NIP

Across the 13 patients, there was no significant relationship between mean FMZ BP_{ND} A/U ratio and mean PK BP_{ND} (A-U) difference within the NIP (Kendall's tau = -0.154, $p=0.464$), see **Figure 3**.

Discussion

This prospective study is the first to assess, in the same subjects, both SNL and MA **and their inter-relationships** in the non-infarcted brain ipsilateral to **MCA stroke**. Consistent with but expanding from earlier reports, FMZ binding was significantly reduced and PK binding significantly increased in the whole non-infarcted MCA territory, for the first time documenting the co-occurrence of MA and SNL beyond the infarct. The focus of this study was however the salvaged penumbra per se. Consistent with our hypothesis, FMZ binding was highly significantly reduced, directly documenting the presence of SNL in the salvaged penumbra in man. Importantly, none of these novel findings could be ascribed to partial volume effects, given the stringent dilated infarct mask approach implemented. Finally, contrary to our hypothesis, **only mild and non-significant increases in PK binding were found in the salvaged penumbra across the sample - although appeared to be present in one patient taken individually**. Finally, there was no significant relationship between FMZ and PK binding changes either in the whole non-infarcted MCA territory or in the salvaged penumbra.

Before addressing the mechanistic implications of these findings, some methodological points deserve comments. First, to identify the penumbra, we applied validated CTP thresholds (Wintermark *et al.*, 2006, Murphy *et al.*, 2008), as previously by us (Alawneh *et al.*, 2011, Carrera *et al.*, 2013). There is currently no consensus on which CTP thresholds to universally apply (Dani *et al.*, 2011, Leigh *et al.*, 2017), and to date numerous CTP thresholds based on different perfusion variables have been validated, though all in single or dual studies only (Wintermark *et al.*, 2006, Murphy *et al.*, 2008, Lin *et al.*, 2014, McVerry *et al.*, 2014, Copen *et al.*, 2015, Cereda *et al.*, 2016, Mokin *et al.*, 2017). Furthermore, in order to identify the penumbra, both penumbral and core perfusion thresholds must be applied, yet the latter is by definition time-dependent (Jones *et al.*, 1981, Baron, 2001), as recently confirmed in stroke patients (d'Esterre *et al.*, 2015, Bivard *et al.*, 2017). Applying the same CTP thresholds as those used here previously yielded biologically meaningful

and expected results, particularly regarding clinical correlations (Alawneh *et al.*, 2011). Furthermore, tissue compartment volumes derived from the various validated thresholds are closely inter-related, and their relationships with clinical or tissue outcome appear stable across thresholds (Christensen *et al.*, 2009, Bivard *et al.*, 2011, Lin *et al.*, 2016). Accordingly, changing the thresholds in sensitivity analyses in our previous study did not affect the overall results (Alawneh *et al.*, 2011). As a matter of fact, the three main CTp variables not only derive from the same contrast agent concentration time-course, but are also mathematically inter-related (i.e., $MTT = CBF/CBV$), so that different thresholds capture widely overlapping voxel subsets. Second, only two CTp slabs were available, so any MA present in cranial- and caudal-most axial sections would have been missed. **Third, we used the specific PET ligands FMZ and PK to investigate SNL and MA, respectively. As FMZ binds selectively to the neuron-specific GABA_A receptor, we were unable to investigate the white matter component of the salvaged penumbra, may have missed SNL affecting non-GABA_A neuronal populations, and, due to locally low GABA_A-receptor density, were unable to investigate striatal SNL, which is commonly seen after brief proximal MCAo in rodents (Fujioka *et al.*, 2003, Katchanov *et al.*, 2003, Baron *et al.*, 2014, Brunner *et al.*, 2017). As a result, we may have underestimated the extent/magnitude of SNL. Regarding PK, it almost exclusively reflects MA (Ejaz *et al.*, 2016) so our findings essentially do not reflect other components of post-stroke inflammation such as astrocytosis and infiltration by blood-borne neutrophils and monocytes. Although PK and FMZ have been formally validated in rodent stroke models as *in vivo* markers of MA and SNL, respectively (see Introduction), direct validation of their intended pathological substrates in humans is available for ³H-labeled PK only (Benavides *et al.*, 1988). Fourth, although sizeable, our sample was relatively small. However i) our FMZ and PK samples taken separately were both larger than any previous similar study (see Introduction); ii) significant FMZ reductions and PK increases were clearly demonstrated despite the relatively small samples; and iii) no previous clinical stroke study has involved both FMZ and PK PET. More generally, assembling a sample of stroke patients with documented acute penumbra, marked early recovery and willingness to undergo two ligand PET studies represents a major achievement - not to mention successfully completing such complex investigations. **However, our findings apply only to patients fulfilling these criteria, and may not generalize to the****

entire stroke population. That said, our sample does reflect current candidates for thrombolysis and bridging therapy.

Although well-established in rodent models (see (Baron *et al.*, 2014) for review), this study is the first to formally document the existence of SNL in the surviving penumbra in man. The only previous similar study that used FMZ in conjunction with acute perfusion imaging documented SNL in the non-infarcted MCA territory but did not directly assess the NIP (Guadagno *et al.*, 2008). Another small-scale FMZ-PET study (Carrera *et al.*, 2013) provided only indirect support to the presence of SNL in the NIP. Two SPECT studies suggested the presence of SNL in the NIP (Nakagawara *et al.*, 1997, Saur *et al.*, 2006) but had significant methodological limitations (see Introduction for details).

In our previous study (Guadagno *et al.*, 2008) the hypothesis that SNL affects the NIP was indirectly tested by assessing the relationship between FMZ binding and acute-stage perfusion across ROIs sampling the affected hemisphere, which revealed the predicted significant negative relationship. Here, in contrast, it was feasible to co-register the PET, MRI and acute-stage CTP datasets, which allowed us to directly document reduced FMZ in the NIP. In a *post-hoc* analysis applying the Guadagno *et al.*'s methodology onto the present material, no significant relationship between FMZ and perfusion was found either within- or across subjects (data not shown). This negative finding may be explained firstly because the present sample had less extensive acute hypoperfusion than in Guadagno *et al.*, reducing the chance of finding a relationship, and secondly because in the latter study the correlations, when significant, had very shallow slopes. Applying the same methodology to the PK dataset, a significant positive PK-perfusion correlation (i.e., in the expected direction) was present in 3/13 patients, but a negative slope was found in 5 patients and the mean slope did not differ from zero. This negative finding is consistent with the lack of significant MA in the NIP, while the presence of MA in the whole non-infarcted MCA mask likely reflects secondary degeneration (see below), whose link with acute hypoperfusion would not be expected.

That the salvaged penumbra can be affected by SNL has potential clinical implications. First, although undetectable on standard MRI (yet possibly identifiable on very-high-field scanners), SNL may contribute to post-stroke neurological

impairment over and above that resulting from the infarct *per se*. Second, SNL may also affect the potential for reorganization and plasticity in the salvaged penumbra, and in turn hinder recovery. Although in rats isolated SNL is associated with sometimes prolonged behavioral impairment (Sicard *et al.*, 2006, Balkaya *et al.*, 2013, Ejaz *et al.*, 2015), only indirect evidence for such an effect exists in man (see Introduction). To test whether SNL impacted recovery (i.e., FMZ-study *minus* admission NIHSS) in the present study, we added SNL severity to our previously validated linear model including salvaged penumbra and extra-penumbra infarct extension (Alawneh *et al.*, 2011, Tisserand *et al.*, 2014), which however failed because 11/16 patients had 100% recovery (see Table 2). Using non-parametric partial correlations to at least partly account for this ceiling effect, salvaged penumbra volume had the expected positive effect on NIHSS recovery, but not SNL (data not shown). However, this ceiling effect prevented the proper testing of this hypothesis. Given the NIHSS only includes major neurological impairments, simple validated assessments of manual dexterity (Calautti *et al.*, 2007) and left- and right-sided MCA stroke-related cognitive deficits (Hillis *et al.*, 2002) were prospectively part of this study's protocol. However, it proved practically impossible to administer them in the hyperacute stroke setting, and eventually this data was available in too few patients for meaningful analysis. These issues notwithstanding, preventing SNL as an adjunct to reperfusion therapies might facilitate and even perhaps enhance ultimate post-stroke recovery.

Our second main hypothesis was that the NIP would also be affected by MA in man. Contrary to this hypothesis, however, our data for the NIP showed only mild and non-significant PK BP_{ND} increases. Rather than a sample size issue, this negative finding might reflect the stringent dilated infarct mask methodology implemented, which, as per our previous study (Price *et al.*, 2006), was necessary because PVEs may cause spill-out of the high PK binding present in necrotic tissue - reflecting massive macrophage-led phagocytosis - onto neighbouring cortex (see Figure 1). Note however that there is currently no alternative to PET to assess MA *in vivo*. Although we cannot formally exclude the presence of MA in the immediate peri-infarct rim, this is a small region that in addition includes the peri-infarct inflammatory scar (Moskowitz *et al.*, 2010), which has no clear clinical relevance. In addition, despite using the same methodology, we did detect the presence of SNL in the NIP, as

predicted, with high statistical significance. Our hypothesis was based on consistent observations in rodents of marked MA in the salvaged penumbra, as biologically expected in close topographical congruence with SNL (Katchanov *et al.*, 2003, Hughes *et al.*, 2010, Ejaz *et al.*, 2013, Ejaz *et al.*, 2015). Given this topographical congruence and the fact that previous clinical FMZ-PET studies have shown cortical SNL to adopt a widely distributed patchy pattern (Guadagno *et al.*, 2008, Carrera *et al.*, 2013), as also found here (Figure 2), one might expect MA to be detectable just as easily as SNL was. Could our negative finding therefore relate to another feature of our study, namely the timing of PK-PET, 14-28 days post-stroke? Time-course studies in rodents have consistently shown prominent MA in the stroke hemisphere from day 3 up to day 28, peaking around day 7-14, and only slightly declining by day 28 (Benavides *et al.*, 1990, Cremer *et al.*, 1992, Fukumoto *et al.*, 2010, Lartey *et al.*, 2014, Walberer *et al.*, 2014, Martin *et al.*, 2015). In baboons, PK binding in the peri-infarct region showed a slightly slower time-course, peaking between days 20-30 (Sette *et al.*, 1993). Acknowledging the complexities involved in carrying out longitudinal PET studies in stroke patients, the available studies suggest a time-course similar to that in baboons (Ramsay *et al.*, 1992, Gerhard *et al.*, 2000, Price *et al.*, 2006). It is therefore unlikely that the peak of MA was missed in the present study. **Taken together, therefore, our study provides strong evidence that MA is not present to any significant amounts in the NIP in man. Interestingly, however, visual inspection of the individual image datasets suggested it was perhaps present in three patients, and more conspicuously in one (see Figure 1). This suggests that although on average MA does not significantly affect the NIP in man, it may be occasionally encountered.**

Consistent with this overall mismatch between SNL and MA in the NIP, there was not even a trend for a correlation between them in this tissue compartment (Figure 3). This negative finding conflicts with our rodent study revealing a significant correlation between SNL and MA, assessed post-mortem at day 14 post-stroke (Hughes *et al.*, 2010), reflecting the above-mentioned topographical congruence between these two processes. It is unlikely this discrepancy resulted from the exclusion of the immediate peri-infarct tissue here, since in man, like in rodents (Sicard *et al.*, 2006, Hughes *et al.*, 2010, Ejaz *et al.*, 2013, Ejaz *et al.*, 2015), cortical

SNL is patchy and widely distributed throughout the MCA territory (see above). A species difference may therefore exist.

In turn our findings provide evidence that MA is unlikely to contribute to any significant degree to the SNL involving the NIP. Although MA is initially triggered by ischemic neuronal injury (Moskowitz *et al.*, 2010), the mismatch and lack of correlation between these two processes found here suggest no lingering relationship between them in man. Our study's clinical implication is therefore that interventions aimed at mitigating MA may not prevent penumbral SNL in man – or at the very least that trials testing this approach should screen for the occasional patients with imaging evidence of both MA and SNL affecting the NIP. Other mechanisms for SNL should therefore be considered. Prominent among them is ischemia-triggered neuronal damage (Guadagno *et al.*, 2008), which if true could be prevented by improving penumbral perfusion or oxygenation until reperfusion is achieved (Shuaib *et al.*, 2011, Ejaz *et al.*, 2016, Poli *et al.*, 2017, Savitz *et al.*, 2017). Another potential mechanism for scattered cortical neuronal death is capillary obstruction - so-called no-reflow –, seemingly caused by pericyte contraction in severely ischemic areas (Yemisci *et al.*, 2009, Dalkara and Arsava, 2012).

Using optimized methodology, the present study confirmed the presence of MA in the non-infarcted MCA territory, previously suggested by two small-scale studies (Gerhard *et al.*, 2005, Price *et al.*, 2006) (see details in Introduction). Furthermore, the lack of significant correlation between FMZ and PK changes in this tissue compartment despite significant changes in both ligands being present suggests topographical non-congruence, with SNL affecting cortical patches and MA being more distributed. As also detailed in Introduction, several clinical studies previously documented MA as a marker of remote degeneration after stroke (Pappata *et al.*, 2000, Gerhard *et al.*, 2005, Radlinska *et al.*, 2009, Thiel *et al.*, 2010). It is likely the presence of MA in the whole non-infarcted MCA territory here reflects similar processes. Whether such remote degeneration is clinically relevant or represents an epiphenomenon is unclear. Some rodent studies suggest that blocking remote inflammation may reduce secondary damage in connected thalamic or brainstem nuclei (see for review (Zhang *et al.*, 2012), with potential behavioural benefits, but others conversely suggest that post-stroke MA has pro-repair effects and that its pharmacological blockade may worsen behavioural outcome (Lalancette-Hebert *et al.*,

2007, Moskowitz *et al.*, 2010, Szalay *et al.*, 2016, Jin *et al.*, 2017). Although this dichotomy and time-course are hotly debated (Ransohoff, 2016), neurotoxic effects may predominate in the first week and pro-repair effects later on (Hu *et al.*, 2012).

Conclusion

The present mechanistic dual-tracer PET study in a sizeable sample of **MCA territory stroke** patients establishes the presence of microglial activation in the non-infarcted MCA territory taken as a whole, uncorrelated with neuronal loss. More important, we demonstrate for the first time the presence of patchy SNL affecting the MR normal-appearing cortical ribbon within the surviving penumbra. The lack of associated microglial activation suggests the latter may not contribute to SNL in human stroke. In turn, the presence of MA in non-infarcted areas probably represents remote degenerative processes rather than potentially neurotoxic inflammation further damaging the penumbra. The main clinical implications from our findings are, first, that SNL affecting the salvaged penumbra may hinder neuronal plasticity and functional recovery, and as such may represent a novel therapeutic target as an adjunct to reperfusion therapies; and, second, that microglial activation may not stand as primary target for interventions aiming to prevent SNL. **Other interventions, such as improving penumbral perfusion/oxygenation before reperfusion is achieved and/or preventing capillary obstruction, may more efficiently prevent SNL. For such trials, FMZ-PET may be of use to monitor treatment effects.**

Acknowledgements: We thank Drs R. Smith, V. Ferrari and N. Antoun, and Mrs ST Marrapu for support, and Dr Guillaume Turc, MD, BA, PhD for statistical advice.

Funding: Work supported by the UK Medical Research Council (grant # G0500874). JA Alawneh was supported by the EU I-KNOW Consortium grant (Grant 027294) and PS Jones by the Cambridge Biomedical Centre grant.

Literature cited

- Alawneh JA, Jones PS, Mikkelsen IK, Cho TH, Siemonsen S, Mouridsen K, et al. Infarction of 'non-core-non-penumbra' tissue after stroke: multivariate modelling of clinical impact. *Brain*. 2011;134(Pt 6):1765-76.
- Arlicot N, Petit E, Katsifis A, Toutain J, Divoux D, Bodard S, et al. Detection and quantification of remote microglial activation in rodent models of focal ischaemia using the TSPO radioligand CLINDE. *European journal of nuclear medicine and molecular imaging*. 2010;37(12):2371-80.
- Balkaya M, Krober J, Gertz K, Peruzzaro S, Endres M. Characterization of long-term functional outcome in a murine model of mild brain ischemia. *J Neurosci Methods*. 2013;213(2):179-87.
- Baron JC. Mapping the ischaemic penumbra with PET: a new approach. *Brain*. 2001;124(Pt 1):2-4.
- Baron JC, Yamauchi H, Fujioka M, Endres M. Selective neuronal loss in ischemic stroke and cerebrovascular disease. *J Cereb Blood Flow Metab*. 2014;34(1):2-18.
- Benavides J, Capdeville C, Dauphin F, Dubois A, Duverger D, Fage D, et al. The quantification of brain lesions with an omega 3 site ligand: a critical analysis of animal models of cerebral ischaemia and neurodegeneration. *Brain Res*. 1990;522(2):275-89.
- Benavides J, Cornu P, Dennis T, Dubois A, Hauw JJ, MacKenzie ET, et al. Imaging of human brain lesions with an omega 3 site radioligand. *Ann Neurol*. 1988;24(6):708-12.
- Bivard A, Kleinig T, Miteff F, Butcher K, Lin L, Levi C, et al. Ischemic core thresholds change with time to reperfusion: A case control study. *Ann Neurol*. 2017;82(6):995-1003.
- Bivard A, Spratt N, Levi C, Parsons M. Perfusion computer tomography: imaging and clinical validation in acute ischaemic stroke. *Brain*. 2011;134(Pt 11):3408-16.
- Brunner C, Isabel C, Martin A, Dussaux C, Savoye A, Emmrich J, et al. Mapping the dynamics of brain perfusion using functional ultrasound in a rat model of transient middle cerebral artery occlusion. *J Cereb Blood Flow Metab*. 2017;37(1):263-76.
- Calautti C, Baron JC. Functional neuroimaging studies of motor recovery after stroke in adults: a review. *Stroke*. 2003;34(6):1553-66.
- Calautti C, Naccarato M, Jones PS, Sharma N, Day DD, Carpenter AT, et al. The relationship between motor deficit and hemisphere activation balance after stroke: A 3T fMRI study. *Neuroimage*. 2007;34(1):322-31.
- Cao Y, Vikingstad EM, George KP, Johnson AF, Welch KM. Cortical language activation in stroke patients recovering from aphasia with functional MRI. *Stroke*. 1999;30(11):2331-40.
- Carrera E, Jones PS, Morris RS, Alawneh J, Hong YT, Aigbirhio FI, et al. Is neural activation within the rescued penumbra impeded by selective neuronal loss? *Brain*. 2013;136(Pt 6):1816-29.
- Cereda CW, Christensen S, Campbell BC, Mishra NK, Mlynash M, Levi C, et al. A benchmarking tool to evaluate computer tomography perfusion infarct core predictions against a DWI standard. *J Cereb Blood Flow Metab*. 2016;36(10):1780-9.
- Christensen S, Mouridsen K, Wu O, Hjort N, Karstoft H, Thomalla G, et al. Comparison of 10 perfusion MRI parameters in 97 sub-6-hour stroke patients using voxel-based receiver operating characteristics analysis. *Stroke*. 2009;40(6):2055-61.
- Copen WA, Morais LT, Wu O, Schwamm LH, Schaefer PW, Gonzalez RG, et al. In Acute Stroke, Can CT Perfusion-Derived Cerebral Blood Volume Maps Substitute for Diffusion-Weighted Imaging in Identifying the Ischemic Core? *PloS one*. 2015;10(7):e0133566.
- Cramer SC, Moore CI, Finklestein SP, Rosen BR. A pilot study of somatotopic mapping after cortical infarct. *Stroke*. 2000;31(3):668-71.
- Cremer JE, Hume SP, Cullen BM, Myers R, Manjil LG, Turton DR, et al. The distribution of radioactivity in brains of rats given [N-methyl-11C]PK 11195 in vivo after induction of a cortical ischaemic lesion. *Int J Rad Appl Instrum B*. 1992;19(2):159-66.

- d'Esterre CD, Boesen ME, Ahn SH, Pordeli P, Najm M, Minhas P, et al. Time-Dependent Computed Tomographic Perfusion Thresholds for Patients With Acute Ischemic Stroke. *Stroke*. 2015;46(12):3390-7.
- Dalkara T, Arsava EM. Can restoring incomplete microcirculatory reperfusion improve stroke outcome after thrombolysis? *J Cereb Blood Flow Metab*. 2012;32(12):2091-9.
- Dani KA, Thomas RG, Chappell FM, Shuler K, MacLeod MJ, Muir KW, et al. Computed tomography and magnetic resonance perfusion imaging in ischemic stroke: definitions and thresholds. *Ann Neurol*. 2011;70(3):384-401.
- Dubois A, Benavides J, Peny B, Duverger D, Fage D, Gotti B, et al. Imaging of primary and remote ischaemic and excitotoxic brain lesions. An autoradiographic study of peripheral type benzodiazepine binding sites in the rat and cat. *Brain Res*. 1988;445(1):77-90.
- Ejaz S, Emmrich JV, Sawiak SJ, Williamson DJ, Baron JC. Cortical selective neuronal loss, impaired behavior, and normal magnetic resonance imaging in a new rat model of true transient ischemic attacks. *Stroke*. 2015;46(4):1084-92.
- Ejaz S, Emmrich JV, Sitnikov SL, Hong YT, Sawiak SJ, Fryer TD, et al. Normobaric hyperoxia markedly reduces brain damage and sensorimotor deficits following brief focal ischaemia. *Brain*. 2016;139(Pt 3):751-64.
- Ejaz S, Williamson DJ, Ahmed T, Sitnikov S, Hong YT, Sawiak SJ, et al. Characterizing infarction and selective neuronal loss following temporary focal cerebral ischemia in the rat: a multi-modality imaging study. *Neurobiol Dis*. 2013;51:120-32.
- Emberson J, Lees KR, Lyden P, Blackwell L, Albers G, Bluhmki E, et al. Effect of treatment delay, age, and stroke severity on the effects of intravenous thrombolysis with alteplase for acute ischaemic stroke: a meta-analysis of individual patient data from randomised trials. *Lancet*. 2014;384(9958):1929-35.
- Fisher M, Saver JL. Future directions of acute ischaemic stroke therapy. *Lancet Neurol*. 2015;14(7):758-67.
- Fujioka M, Taoka T, Matsuo Y, Mishima K, Ogoshi K, Kondo Y, et al. Magnetic resonance imaging shows delayed ischemic striatal neurodegeneration. *Ann Neurol*. 2003;54(6):732-47.
- Fukumoto D, Hosoya T, Nishiyama S, Harada N, Iwata H, Yamamoto S, et al. Multiparametric assessment of acute and subacute ischemic neuronal damage: A small animal positron emission tomography study with rat photochemically induced thrombosis model. *Synapse*. 2010.
- Funck T, Al-Kuwaiti M, Lepage C, Zepper P, Minuk J, Schipper HM, et al. Assessing neuronal density in peri-infarct cortex with PET: Effects of cortical topology and partial volume correction. *Hum Brain Mapp*. 2017;38(1):326-38.
- Furlan M, Marchal G, Viader F, Derlon JM, Baron JC. Spontaneous neurological recovery after stroke and the fate of the ischemic penumbra. *Ann Neurol*. 1996;40(2):216-26.
- Gerhard A, Neumaier B, Elitok E, Glatting G, Ries V, Tomczak R, et al. In vivo imaging of activated microglia using [¹¹C]PK11195 and positron emission tomography in patients after ischemic stroke. *Neuroreport*. 2000;11(13):2957-60.
- Gerhard A, Schwarz J, Myers R, Wise R, Banati RB. Evolution of microglial activation in patients after ischemic stroke: a [¹¹C](R)-PK11195 PET study. *Neuroimage*. 2005;24(2):591-5.
- Goyal M, Menon BK, van Zwam WH, Dippel DW, Mitchell PJ, Demchuk AM, et al. Endovascular thrombectomy after large-vessel ischaemic stroke: a meta-analysis of individual patient data from five randomised trials. *Lancet*. 2016;387(10029):1723-31.
- Guadagno JV, Jones PS, Aigbirhio FI, Wang D, Fryer TD, Day DJ, et al. Selective neuronal loss in rescued penumbra relates to initial hypoperfusion. *Brain*. 2008;131(Pt 10):2666-78.
- Gunn RN, Lammertsma AA, Hume SP, Cunningham VJ. Parametric imaging of ligand-receptor binding in PET using a simplified reference region model. *Neuroimage*. 1997;6(4):279-87.

- Heiss WD, Grond M, Thiel A, von Stockhausen HM, Rudolf J, Ghaemi M, et al. Tissue at risk of infarction rescued by early reperfusion: a positron emission tomography study in systemic recombinant tissue plasminogen activator thrombolysis of acute stroke. *J Cereb Blood Flow Metab.* 1998;18(12):1298-307.
- Hillis AE, Wityk RJ, Barker PB, Beauchamp NJ, Gailloud P, Murphy K, et al. Subcortical aphasia and neglect in acute stroke: the role of cortical hypoperfusion. *Brain.* 2002;125(Pt 5):1094-104.
- Hu X, Li P, Guo Y, Wang H, Leak RK, Chen S, et al. Microglia/macrophage polarization dynamics reveal novel mechanism of injury expansion after focal cerebral ischemia. *Stroke.* 2012;43(11):3063-70.
- Hughes JL, Beech JS, Jones PS, Wang D, Menon DK, Baron JC. Mapping selective neuronal loss and microglial activation in the salvaged neocortical penumbra in the rat. *Neuroimage.* 2010;49(1):19-31.
- Hughes JL, Jones PS, Beech JS, Wang D, Menon DK, Aigbirhio FI, et al. A microPET study of the regional distribution of [11C]-PK11195 binding following temporary focal cerebral ischemia in the rat. Correlation with post mortem mapping of microglia activation. *Neuroimage.* 2012;59(3):2007-16.
- Jaillard A, Martin CD, Garambois K, Lebas JF, Hommel M. Vicarious function within the human primary motor cortex? A longitudinal fMRI stroke study. *Brain.* 2005;128(Pt 5):1122-38.
- Jin WN, Shi SX, Li Z, Li M, Wood K, Gonzales RJ, et al. Depletion of microglia exacerbates postischemic inflammation and brain injury. *J Cereb Blood Flow Metab.* 2017;37(6):2224-36.
- Jones TH, Morawetz RB, Crowell RM, Marcoux FW, FitzGibbon SJ, DeGirolami U, et al. Thresholds of focal cerebral ischemia in awake monkeys. *J Neurosurg.* 1981;54(6):773-82.
- Katchanov J, Waeber C, Gertz K, Gietz A, Winter B, Bruck W, et al. Selective neuronal vulnerability following mild focal brain ischemia in the mouse. *Brain Pathol.* 2003;13(4):452-64.
- Kaushal V, Schlichter LC. Mechanisms of microglia-mediated neurotoxicity in a new model of the stroke penumbra. *J Neurosci.* 2008;28(9):2221-30.
- Kriz J, Lalancette-Hebert M. Inflammation, plasticity and real-time imaging after cerebral ischemia. *Acta Neuropathol.* 2009;117(5):497-509.
- Lalancette-Hebert M, Gowing G, Simard A, Weng YC, Kriz J. Selective ablation of proliferating microglial cells exacerbates ischemic injury in the brain. *J Neurosci.* 2007;27(10):2596-605.
- Lammertsma AA, Hume SP. Simplified reference tissue model for PET receptor studies. *Neuroimage.* 1996;4(3 Pt 1):153-8.
- Lartey FM, Ahn GO, Shen B, Cord KT, Smith T, Chua JY, et al. PET imaging of stroke-induced neuroinflammation in mice using [18F]PBR06. *Molecular imaging and biology : MIB : the official publication of the Academy of Molecular Imaging.* 2014;16(1):109-17.
- Leigh R, Knutsson L, Zhou J, van Zijl PC. Imaging the physiological evolution of the ischemic penumbra in acute ischemic stroke. *J Cereb Blood Flow Metab.* 2017;271678X17700913.
- Li F, Han SS, Tatlisumak T, Liu KF, Garcia JH, Sotak CH, et al. Reversal of acute apparent diffusion coefficient abnormalities and delayed neuronal death following transient focal cerebral ischemia in rats. *Ann Neurol.* 1999;46(3):333-42.
- Lin L, Bivard A, Krishnamurthy V, Levi CR, Parsons MW. Whole-Brain CT Perfusion to Quantify Acute Ischemic Penumbra and Core. *Radiology.* 2016;279(3):876-87.
- Lin L, Bivard A, Levi CR, Parsons MW. Comparison of computed tomographic and magnetic resonance perfusion measurements in acute ischemic stroke: back-to-back quantitative analysis. *Stroke.* 2014;45(6):1727-32.
- Martin A, Szczupak B, Gomez-Vallejo V, Domercq M, Cano A, Padro D, et al. In vivo PET imaging of the alpha4beta2 nicotinic acetylcholine receptor as a marker for brain inflammation after cerebral ischemia. *J Neurosci.* 2015;35(15):5998-6009.

- McVerry F, Dani KA, MacDougall NJ, MacLeod MJ, Wardlaw J, Muir KW. Derivation and evaluation of thresholds for core and tissue at risk of infarction using CT perfusion. *J Neuroimaging*. 2014;24(6):562-8.
- Mokin M, Levy EI, Saver JL, Siddiqui AH, Goyal M, Bonafe A, et al. Predictive Value of RAPID Assessed Perfusion Thresholds on Final Infarct Volume in SWIFT PRIME (Solitaire With the Intention for Thrombectomy as Primary Endovascular Treatment). *Stroke*. 2017;48(4):932-8.
- Moskowitz MA, Lo EH, Iadecola C. The science of stroke: mechanisms in search of treatments. *Neuron*. 2010;67(2):181-98.
- Muir KW, Buchan A, von Kummer R, Rother J, Baron JC. Imaging of acute stroke. *Lancet Neurol*. 2006;5(9):755-68.
- Murphy BD, Fox AJ, Lee DH, Sahlas DJ, Black SE, Hogan MJ, et al. White matter thresholds for ischemic penumbra and infarct core in patients with acute stroke: CT perfusion study. *Radiology*. 2008;247(3):818-25.
- Myers R, Manjil LG, Cullen BM, Price GW, Frackowiak RS, Cremer JE. Macrophage and astrocyte populations in relation to [3H]PK 11195 binding in rat cerebral cortex following a local ischaemic lesion. *J Cereb Blood Flow Metab*. 1991;11(2):314-22.
- Nakagawara J, Sperling B, Lassen NA. Incomplete brain infarction of reperfused cortex may be quantitated with iomazenil. *Stroke*. 1997;28(1):124-32.
- Nudo RJ. Mechanisms for recovery of motor function following cortical damage. *Curr Opin Neurobiol*. 2006;16(6):638-44.
- Pappata S, Levasseur M, Gunn RN, Myers R, Crouzel C, Syrota A, et al. Thalamic microglial activation in ischaemic stroke detected in vivo by PET and [11C]PK11195. *Neurology*. 2000;55:1052-4.
- Pappata S, Levasseur M, Gunn RN, Myers R, Crouzel C, Syrota A, et al. Thalamic microglial activation in ischemic stroke detected in vivo by PET and [11C]PK11195. *Neurology*. 2000;55(7):1052-4.
- Poli S, Baron JC, Singhal AB, Hartig F. Normobaric hyperoxygenation: a potential neuroprotective therapy for acute ischemic stroke? *Expert Rev Neurother*. 2017;17(12):1131-4.
- Price CJ, Wang D, Menon DK, Guadagno JV, Cleij M, Fryer T, et al. Intrinsic activated microglia map to the peri-infarct zone in the subacute phase of ischemic stroke. *Stroke*. 2006;37(7):1749-53.
- Radlinska BA, Ghinani SA, Lyon P, Jolly D, Soucy JP, Minuk J, et al. Multimodal microglia imaging of fiber tracts in acute subcortical stroke. *Ann Neurol*. 2009;66(6):825-32.
- Ramsay SC, Weiller C, Myers R, Cremer JE, Luthra SK, Lammertsma AA, et al. Monitoring by PET of macrophage accumulation in brain after ischaemic stroke. *Lancet*. 1992;339(8800):1054-5.
- Ransohoff RM. A polarizing question: do M1 and M2 microglia exist? *Nature neuroscience*. 2016;19(8):987-91.
- Rupalla K, Allegrini PR, Sauer D, Wiessner C. Time course of microglia activation and apoptosis in various brain regions after permanent focal cerebral ischemia in mice. *Acta neuropathologica*. 1998;96(2):172-8.
- Saur D, Buchert R, Knab R, Weiller C, Rother J. Iomazenil-Single-Photon Emission Computed Tomography Reveals Selective Neuronal Loss in Magnetic Resonance-Defined Mismatch Areas. *Stroke*. 2006;37(11):2713-9.
- Saver JL. Optimal end points for acute stroke therapy trials: best ways to measure treatment effects of drugs and devices. *Stroke*. 2011;42(8):2356-62.
- Savitz SI, Baron JC, Yenari MA, Sanossian N, Fisher M. Reconsidering Neuroprotection in the Reperfusion Era. *Stroke*. 2017;48(12):3413-9.
- Schwartz M. Macrophages and microglia in central nervous system injury: are they helpful or harmful? *J Cereb Blood Flow Metab*. 2003;23(4):385-94.

- Sette G, Baron JC, Young AR, Miyazawa H, Tillet I, Barre L, et al. In vivo mapping of brain benzodiazepine receptor changes by positron emission tomography after focal ischemia in the anesthetized baboon. *Stroke*. 1993;24(12):2046-57; discussion 57-8.
- Shuaib A, Butcher K, Mohammad AA, Saqqur M, Liebeskind DS. Collateral blood vessels in acute ischaemic stroke: a potential therapeutic target. *Lancet Neurol*. 2011;10(10):909-21.
- Sicard KM, Henninger N, Fisher M, Duong TQ, Ferris CF. Differential recovery of multimodal MRI and behavior after transient focal cerebral ischemia in rats. *J Cereb Blood Flow Metab*. 2006;26(11):1451-62.
- Sicard KM, Henninger N, Fisher M, Duong TQ, Ferris CF. Long-term changes of functional MRI-based brain function, behavioral status, and histopathology after transient focal cerebral ischemia in rats. *Stroke*. 2006;37(10):2593-600.
- Signorini M, Paulesu E, Friston K, Perani D, Colleluori A, Lucignani G, et al. Rapid assessment of regional cerebral metabolic abnormalities in single subjects with quantitative and nonquantitative [¹⁸F]FDG PET: A clinical validation of statistical parametric mapping. *NeuroImage*. 1999;9(1):63-80.
- Stephenson DT, Schober DA, Smalstig EB, Mincy RE, Gehlert DR, Clemens JA. Peripheral benzodiazepine receptors are colocalized with activated microglia following transient global forebrain ischemia in the rat. *J Neurosci*. 1995;15(7 Pt 2):5263-74.
- Szalay G, Martinecz B, Lenart N, Kornyei Z, Orsolits B, Judak L, et al. Microglia protect against brain injury and their selective elimination dysregulates neuronal network activity after stroke. *Nature communications*. 2016;7:11499.
- Tamura A, Tahira Y, Nagashima H, Kirino T, Gotoh O, Hojo S, et al. Thalamic atrophy following cerebral infarction in the territory of the middle cerebral artery. *Stroke*. 1991;22(5):615-8.
- Thiel A, Radlinska BA, Paquette C, Sidel M, Soucy JP, Schirmacher R, et al. The temporal dynamics of poststroke neuroinflammation: a longitudinal diffusion tensor imaging-guided PET study with ¹¹C-PK11195 in acute subcortical stroke. *J Nucl Med*. 2010;51(9):1404-12.
- Tisserand M, Seners P, Turc G, Legrand L, Labeyrie MA, Charron S, et al. Mechanisms of unexplained neurological deterioration after intravenous thrombolysis. *Stroke*. 2014;45(12):3527-34.
- Videbaek C, Andersen JV, Dalgaard L, Foged C, Paulson OB, Lassen AN. Neuroreceptor quantification in vivo by the steady state principle and [¹²³I]iomazenil in rats. *Eur J Pharmacol*. 1995;281(2):117-22.
- Videbaek C, Friberg L, Holm S, Wammen S, Foged C, Andersen JV, et al. Benzodiazepine receptor equilibrium constants for flumazenil and midazolam determined in humans with the single photon emission computer tomography tracer [¹²³I]iomazenil. *Eur J Pharmacol*. 1993;249(1):43-51.
- Walberer M, Jantzen SU, Backes H, Rueger MA, Keuters MH, Neumaier B, et al. In-vivo detection of inflammation and neurodegeneration in the chronic phase after permanent embolic stroke in rats. *Brain Res*. 2014;1581:80-8.
- Wegener S, Weber R, Ramos-Cabrer P, Uhlenkueken U, Sprenger C, Wiedermann D, et al. Temporal profile of T2-weighted MRI distinguishes between pannecrosis and selective neuronal death after transient focal cerebral ischemia in the rat. *J Cereb Blood Flow Metab*. 2006;26(1):38-47.
- Wintermark M, Flanders AE, Velthuis B, Meuli R, van Leeuwen M, Goldsher D, et al. Perfusion-CT assessment of infarct core and penumbra: receiver operating characteristic curve analysis in 130 patients suspected of acute hemispheric stroke. *Stroke*. 2006;37(4):979-85.
- Yemisci M, Gursoy-Ozdemir Y, Vural A, Can A, Topalkara K, Dalkara T. Pericyte contraction induced by oxidative-nitrative stress impairs capillary reflow despite successful opening of an occluded cerebral artery. *Nat Med*. 2009;15(9):1031-7.

Zhang J, Zhang Y, Xing S, Liang Z, Zeng J. Secondary neurodegeneration in remote regions after focal cerebral infarction: a new target for stroke management? *Stroke*. 2012;43(6):1700-5.

For Peer Review

Figure legends

Figure 1

Illustrative image dataset (patient 2). Overlaid on the one-month FLAIR image are shown the infarct ROI and 14-mm dilated infarct ROI (red and blue contours, respectively; note that the Infarct ROI includes the caudate head, which is visible on the FLAIR image). To the left are shown the co-registered non-contrast CT and CTp scans (MTT map) obtained on this patient's admission. Red arrows on the MTT map point to acute-stage penumbral areas. On the right are shown the co-registered FMZ and PK BP_{ND} maps. Visual inspection indicates a clear reduction in FMZ BP_{ND} (red arrows) together with increased PK BP_{ND} (yellow arrows) within the non-infarcted penumbra (and outside the dilated infarct ROI). Note also the massive PK11195 uptake within the infarcted area (blue arrowhead). Refer to Tables 3 and 4 for individual FMZ and PK BP_{ND} values in the non-infarcted MCA territory and non-infarcted penumbra (NIP) in this patient. Consistent with these visual observations, this patient had the second lowest FMZ (A/U) ratio and highest (A-U) PK difference in the NIP.

Figure 2

Illustrative SPM readouts from Patient 2 (same patient as in Figure 1) showing, projected onto 5 axial cuts from a normal T1-MRI template for anatomical orientation, typical clusters of significant FMZ binding reduction (as compared to 12 healthy controls, see Methods) scattered across the right MCA-territory cortical ribbon (yellow blobs), i.e., ipsilateral to the stroke, with only few similar clusters on the left cortical ribbon (blue blobs; see Methods for an explanation as to how and why such clusters were identified in the unaffected hemisphere). Quantitative FMZ data for this patient are shown in Table 3.

Figure 3

Scatterplot of the relationship between FMZ affected/unaffected (A/U) side ratio and PK (A-U) side difference for the non-infarcted penumbra (see Methods). This plot shows no clear relationship between the two variables, which was confirmed by the statistical analysis (Kendall's tau = -0.154, p = 0.464). Note that Kendall's rank correlation corrects for any potential outlier. Note also the data point at the bottom

right corner of the sample, ie, with highest PK value and the second lowest FMZ value in the NIP, corresponds to Patient 2, in whom visual inspection of the image dataset suggested the presence of increased PK binding in the NIP (see Figure 1).

For Peer Review

Table 1. Summary of demographics

Patient	Gender	Age (yrs)	Hemisphere affected	HTN	DM	Hyper-Cholesterol aemia	Current smoking history	rt-PA given	Cause of stroke§
1	F	61	L	○	○	○	○	Y	3
2	F	74	R	○	○	○	○	Y	5
3	M	54	R	●	○	○	●	Y	2
4	M	49	L	○	○	○	○	Y	3
5	F	74	L	●	○	○	○	Y	3
6	F	80	R	○	○	○	○	Y	3
7	M	56	L	○	○	●	○	Y	3
8	M	55	L	●	○	○	●	Y	3
9	F	71	R	○	○	○	○	Y	3
10	M	64	R	○	○	○	○	Y	2
11	M	59	R	○	○	○	○	Y	3
12	M	87	L	●	○	○	○	N	3
13	M	68	L	●	○	○	○	N	3
14	M	53	R	○	○	○	○	Y	5
15	M	74	R	●	●	●	○	N	2
16	F	76	L	●	○	●	○	Y	5

L: left; R: right; HTN : hypertension, DM : diabetes mellitus; ● present ○ absent ; §TOAST criteria 1: Severe carotid stenosis, 2: Large artery disease, 3: Cardioembolic cause, 4: Other determined cause, 5: Undetermined

Table 2. PET data acquisition delays, NIHSS data and infarct volume for the 16 patients recruited into the present study (#1-16) and the two additional PK patients from Price et al, 2006.

Patient	Stroke onset to CT (mins)	Initial NIHSS	24hr NIHSS	Interval to PK scan (days)	NIHSS at PK scan	Interval to FMZ scan (days)	NIHSS at FMZ scan	Infarct volume (ml)&
1	109	4	2	24	1	43	1	11.0
2	91	18	10	18	10	50	10	14.1
3	89	20	3	17	2	100	2	98.5
4	191	4	0	21	0	146	0	2.0
5	148	21	3	16	3	147	3	11.5
6	131	19	0	13	0	48	0	31.3
7	140	3	0	27	0	119	0	0.3
8	94	5	0	15	0	47	0	1.3
9	147	15	0	21	0	58	0	0.7
10	142	11	0	22	0	84	0	5.1
11	83	7	2	16	0	92	0	0.2
12	312*	13	1	26	1	104	1	3.0
13	142	5	1	26	1	89	0	5.2
14	234	2	0	n/a	n/a	41	0	6.0
15	145	6	1	n/a	n/a	116	0	54.6
16	118	8	1	13	1	n/a	n/a	7.0
17 ^a	n/a	19	10	13	n/a	n/a	n/a	25.3
18 ^a	n/a	13	1	25	n/a	n/a	n/a	2.7

CT: computerized tomography; *interval calculated from when last seen well; &: total infarct volume across the whole brain, obtained at FMZ session whenever applicable, otherwise at PK session (see Methods); a: these two patients were initially reported in Price et al (Price *et al.*, 2006), see Methods for details; n/a – not available/not applicable.

Table 3. Number of statistically significant FMZ voxels in the non-infarcted MCA and mirror masks, corresponding PK ratios, and (affected minus unaffected) (A – U) difference in these variables, for each of the 16 patients included in the present study plus the two PK patients from Price et al 2006. See Methods for details and Results for statistical findings.

Patient	FMZ affected hemisphere	FMZ unaffected hemisphere	FMZ (A – U) difference	PK ratio affected hemisphere (%)	PK ratio unaffected hemisphere (%)	PK ratio (A – U) Difference (%)
1	480	200	280	1.13	0.38	0.75*
2	2393	1286	1107	3.00	2.24	0.74*
3	0	111	-111	9.05	7.67	1.38*
4	0	0	0	2.31	1.58	0.73*
5	101	0	101	2.04	3.38	-1.34
6	0	0	0	0.52	0.64	-0.12
7	0	0	0	4.32	3.90	0.42*
8	368	0	368	6.62	7.19	-0.57
9	303	532	-229	2.01	1.51	0.50*
10	0	0	0	0.30	0.36	-0.06
11	0	0	0	0.89	0.75	0.14
12	4768	2296	2472	0.80	0.36	0.44*
13	0	0	0	2.39	1.67	0.72*
14	895	0	895	n/a	n/a	n/a
15	345	0	345	n/a	n/a	n/a
16	n/a	n/a	n/a	2.46	1.17	1.29*
17	n/a	n/a	n/a	4.45	2.86	1.59*
18	n/a	n/a	n/a	1.01	0.42	0.59*

*: value higher than the upper 95% confidence limit for the inter-hemispheric difference in PK ratio derived from the 10 control subjects who underwent a PK PET study (value: 0.35%).

Table 4. Mean FMZ and PK BP_{ND} values within the non-infarcted penumbra and mirror masks, and their corresponding A/U ratio and (A-U) difference, respectively, in the 16 patients recruited in the present study. Also shown is the volume of non-infarcted penumbra, assessed in two CT perfusion slices. See Methods for details and Results for statistical findings.

Patient	FMZ Affected	FMZ Unaffected	FMZ (A/U) ratio	PK Affected	PK Unaffected	PK (A-U) difference	Salvaged penumbra volume (mls)
1	2.030	2.032	0.999	-0.097	-0.116	0.019	92.3
2	2.764	3.377	0.818	-0.032	-0.137	0.105	62.1
3	2.647	3.023	0.876	-0.024	-0.070	0.046	53.3
4	2.188	2.359	0.927	-0.063	-0.089	0.026	24.1
5	3.119	3.555	0.878	-0.053	-0.028	-0.024	26.3
6	2.782	3.153	0.883	-0.088	-0.086	-0.002	46.6
7	2.304	2.801	0.823	-0.151	-0.126	-0.025	34.6
8	2.165	2.325	0.931	-0.112	-0.115	0.004	31.1
9	2.221	2.339	0.950	-0.060	-0.053	-0.007	71.2
10	2.495	2.582	0.966	-0.134	-0.118	-0.016	40.1
11	3.100	3.253	0.953	-0.128	-0.138	0.011	75.9
12	2.900	3.623	0.800	-0.037	-0.102	0.065	24.0
13	2.880	3.485	0.827	-0.143	-0.144	0.001	56.6
14	4.182	4.540	0.921	n/a	n/a	n/a	96.6
15	3.369	4.023	0.838	n/a	n/a	n/a	24.6
16	n/a	n/a	n/a	-0.099	-0.117	0.018	48.9

n/a: not available

Figure 1

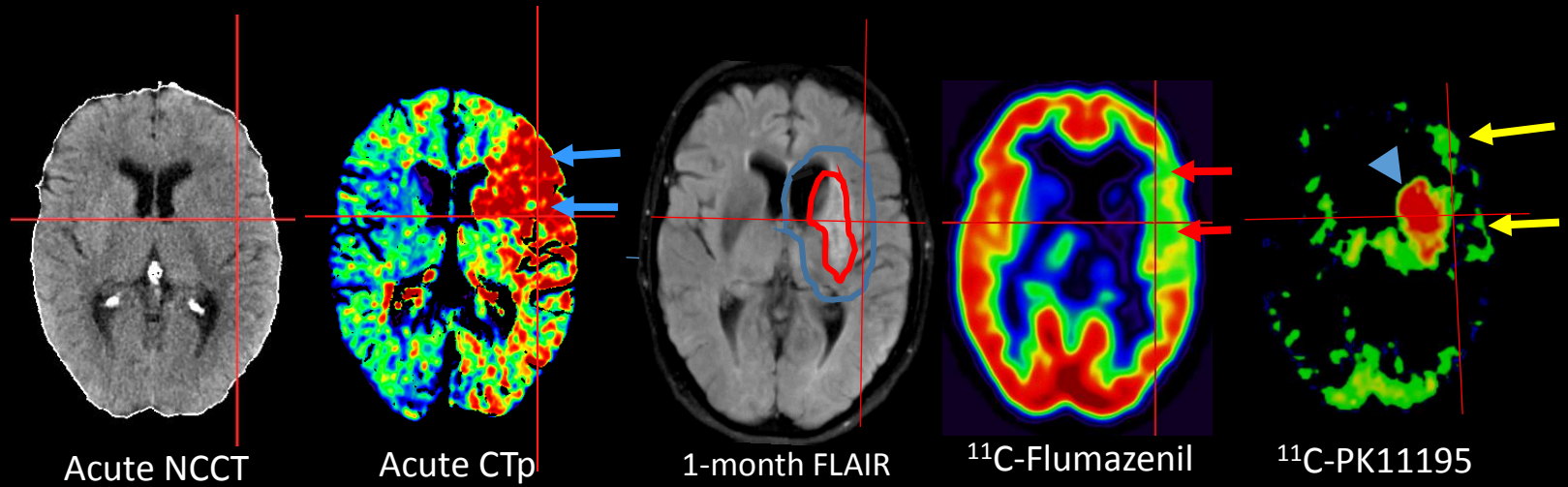


Figure 2

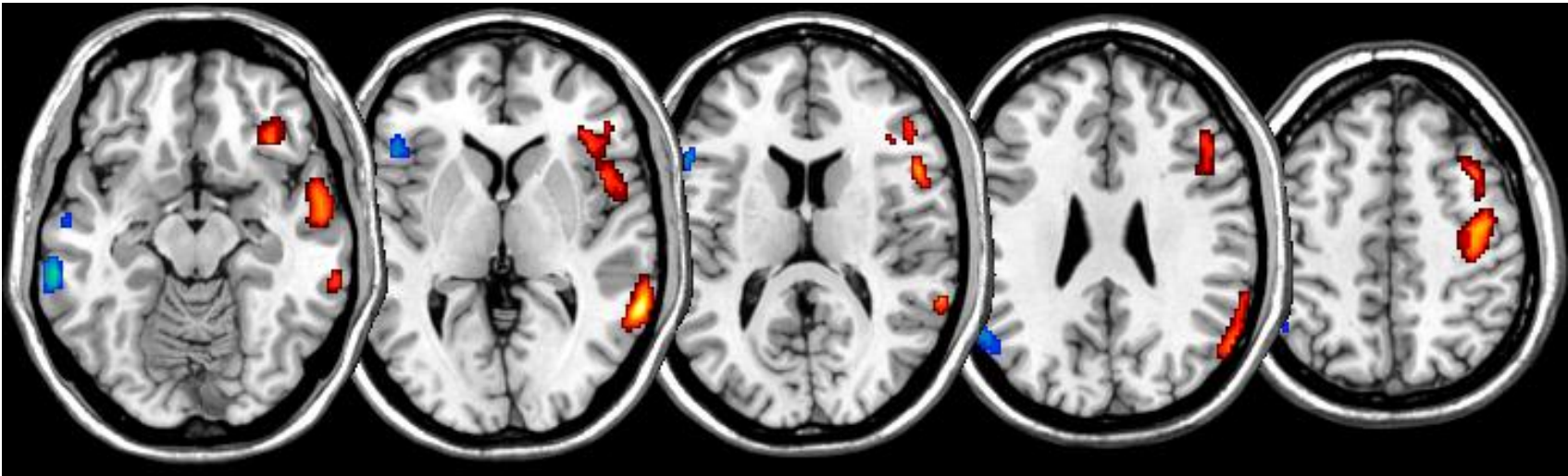


Figure 3

